DOI: 10.53469/jpce.2026.08(02).05

Application of Comprehensive Investigation Methods in Seepage Diagnosis and Prediction of a Clay Core Rockfill Dam

Jinhang Yin*, Bei Su

China Water Resources & Hydropower Engineering BOHAI Consultancy Co, Tianjin 300222, China
Correspondence Author, dahang64@163.com

Abstract: ***Aiming at the problem of intensified downstream seepage in a clay core gravelly soil dam after impoundment, this study adopted a comprehensive approach that integrated surface observation, high-density electrical resistivity tomography, self-potential method, tracer tests, and itemized seepage calculation. The investigation revealed that the seepage is primarily controlled by defects in the concrete cutoff wall of the dam foundation and the heterogeneous permeability of the clay core. Key permeability parameters were obtained through inversion of observed data, and the seepage discharge at different water levels was calculated item by item using Darcy's law. The results show that under the current water level, the measured total seepage discharge is 103.64 L/s, while the calculated value is 100.54 L/s, yielding an error of only 3.08%. This close agreement verifies the reliability of the derived parameters and the applied methodology. The total seepage discharge is predicted to reach 241.28 L/s at the normal impoundment level. This research provides a direct basis for the danger elimination and reinforcement of the dam. The integrated diagnostic and verification methodology developed in this study can serve as a valuable reference for investigating seepage in similar earth-rock dams.***

Keywords: Dam seepage, Seepage mode, Seepage cause, Seepage prediction, Clay core**.**

1. Introduction

The reservoir was constructed in 2012, and the dam is a clay core gravelly soil dam. Seepage control is achieved using a clay core within the dam body and a concrete cutoff wall in the foundation. Following reservoir impoundment, multiple seepage points were observed at the base of the downstream drainage prism, with particularly noticeable flow on the upstream side of the drainage ditch. Both the number of seepage points and the total discharge increased with rising reservoir water levels.

Based on previously published papers and literature, research on seepage in earth-rock dams has largely been conducted using geophysical methods. Examples include the application of high-density electrical resistivity, the use of ground-penetrating radar in studying dam seepage issues (Qiu, 2025; Liu et al, 2024;Yao et al, 2024), diagnostic studies using combined wave velocity-resistivity imaging (Zhao et al, 2012), research on the distribution patterns of electric fields in seepage channels (Wang, 2019), diagnostic studies with three-dimensional resistivity imaging (Zhang et al, 2016), the use of infrared thermal imaging technology to detect concentrated seepage in earth-rock dams (Peng et al, 2016), and research on identifying hidden seepage hazards in reservoir dams and embankments based on time-domain transient electromagnetic methods (Zhang et al, 2025), among others.

The primary advantages of these approaches are their non-destructive nature and relatively low cost and field effort. However, significant limitations exist: geophysical results are influenced by topography, environmental noise, project scale, hydrogeological conditions, and their interpretation is often non-unique and difficult to verify directly.

Therefore, this study adopts a comprehensive investigation framework. It involves rapid scanning of potential anomaly areas using surface geophysical methods, followed by precise verification and parameter acquisition through borehole coring, water pressure tests, and borehole camera surveys. Finally, seepage discharge observations and theoretical calculations are used for cross-verification. This framework aims to establish a more reliable analytical pathway for determining the causes of seepage.

2. Geological Conditions

The strata in the dam site area consist mainly of Neogene sedimentary rocks and Quaternary loose deposits, described from oldest to newest as follows:

(1) Neogene (N_2): Composed mainly of sandy conglomerate, sandstone, and mudstone, with a thickness of 5–30 m. The strata present in brownish-red, grayish-yellow, and grayish-white colors. They are distributed at the right abutment and spillway, mostly covered on the surface but exposed in gullies.

(2) Quaternary Holocene (Q_4): Lithologies include silty sand, silt, low-plasticity clay, and silty gravel, with a thickness of 5–30 m. The thickness at the riverbed ranges from 8.1 to 18.2 m. These deposits are distributed over bedrock surfaces and in the right bank and riverbed, formed by residual, slope wash, alluvial, diluvial, marsh, and artificial processes.

The muddy clay layer in the dam foundation was excavated and replaced with compacted gravelly soil as a treatment measure. Seepage prevention in the permeable gravelly soil layer was achieved using a concrete cutoff wall. Pre-embedded grouting steel pipes were installed within the wall at 2.0 m intervals, allowing for subsequent curtain grouting into the underlying potash feldspar gneiss. The cutoff wall, with a thickness of 0.6 m, extends 2.0 m upwards into the clay core and is embedded 1 m downwards into the underlying potash feldspar gneiss. Based on the seepage range

revealed in the geological longitudinal section, the treatment length of the cutoff wall is 498.87 m. Curtain grouting was also applied to the left and right abutment slopes, with a single row of grouting holes spaced at 2.0 m.

3. Dam Conditions

The dam is a clay core rockfill dam. The core is composed of sandy low-plasticity clay, with a design crest elevation of 1257.12 m, a crest width of 5 m, and a maximum base width of 13.566 m. During the investigation, 70 undisturbed and 12 disturbed soil samples were collected from 8 boreholes along the dam axis.

Laboratory tests yielded the following geotechnical properties for the core clay. The wet density ranged from 1.77 to 2.19 g/cm^3, averaging 2.05 g/cm^3, while the dry density ranged from 1.54 to 1.92 g/cm^3, averaging 1.76 g/cm^3. The void ratio varied between 0.398 and 0.759, with an average of 0.539. The plasticity index ranged from 6.8 to 26.8 (avg. 13.7). The clay content was between 2.5% and 28.9% (avg. 20.7%), and the silt content ranged from 31.40% to 74.10% (avg. 59.9%). The material exhibited medium compressibility, with a compression coefficient ranging from 0.039 to 0.379 MPa^{-1} (avg. 0.156 MPa^{-1}) and a compression modulus between 4.56 and 36.94 MPa (avg. 13.12 MPa).

In terms of mechanical properties, saturated consolidated quick shear tests gave a cohesion ranging from 1.60 to 106.63 kPa (avg. 30.72 kPa) and an internal friction angle between 14.7° and 40.4° (avg. 28.5°). The horizontal permeability coefficient (k) varied widely, from 1.66×10^{-7} to 1.85×10^{-4} cm/s, with an average of 2.78×10^{-5} cm/s. Among the 50 permeability tests, 6 groups exhibited medium permeability, 16 groups weak permeability, and 28 groups very low permeability. The organic matter content ranged from 2.7 to 14.4 g/kg, and the maximum dry density from standard Proctor compaction tests was 1.85 g/cm^3.

4. Evaluation of Dam Fill Quality

Regarding permeability, the horizontal permeability coefficient of the core clay ranges from 1.66×10^{-7} to 1.85×10^{-4} cm/s, averaging 2.78×10^{-5} cm/s. Most values fall within the weak to very low permeability range. However, 44% of the tested samples exceeded the code requirement of 1×10^{-5} cm/s, while 17 groups were below the specified permeability criterion (design standard) of 3.6×10^{-6} cm/s.

Analysis of borehole cores and shaft excavations revealed significant heterogeneity in the permeability of the core clay. Locally high silt content (31.4%–71.2%) was observed, and there was sporadic distribution of low-plasticity silt (e.g., at borehole S6). In these localized areas, the clay content ranged from 2.50% to 4.30%, which is below the code requirement of 15%–40%.

5. Analysis of Geophysical and Tracer Test Results

5.1 High-density Resistivity Tests:

The results show widespread low-resistivity zones in the dam foundation. These zones appear particularly as bead-like distributions in the berm profiles, indicating an uneven but prevalent distribution of permeable layers underground.

5.2 Self-potential Tests:

The inferred groundwater flow directions showed variation along the dam axis:

-In the section from stake 0+000 to 0+060, flow was essentially perpendicular to the dam axis from upstream to downstream.

- From stake 0+060 to 0+170, the flow generally exhibited a shift from the left towards the right.

-From stake 0+170 to 0+240, the flow was again essentially perpendicular.

-From stake 0+240 to 0+480, the flow mostly shifted from the right towards the left.

5.3 Tracer Test Results:

1) The tests confirmed that reservoir water can seep through the dam foundation's seepage control system to the downstream side. This indicates seepage issues in the strata near the bedrock surface, which is consistent with the numerous outflow points observed in the downstream drainage ditch.

2) The relatively faint appearance of the red dye in observation holes was attributed to the adsorption and filtration capacity of the foundation materials. This was later corroborated when flushing the injection holes, as the dye concentration inside remained high.

3) When saline water was used as a tracer in two boreholes, no distinct anomalies were detected downstream. This may be due to the rapid diffusion and dilution of saline water upon injection into the reservoir, aided by mixing. Additionally, the seepage is not a conduit-type flow, which further favors diffusion and dilution, explaining the lack of a clear signal in downstream observation holes.

6. Observation and Analysis of Downstream Seepage Discharge

6.1 Observation of Seepage Points

Field surveys identified 25 distinct seepage points at the toe of the downstream drainage prism, with 4 points having relatively large discharges. At some points, fine sand was observed being carried and churned by the seepage flow. The seepage water appeared clear and transparent (Figure 1), with no turbidity observed, indicating no active seepage deformation (piping) issues in the dam foundation.

Furthermore, several large water-filled depressions exist downstream of the dam (Figure 2), which collect seepage water and form surface flow that discharges along the main river channel.

Figure 1: Seepage in the drainage ditch downstream of the dam

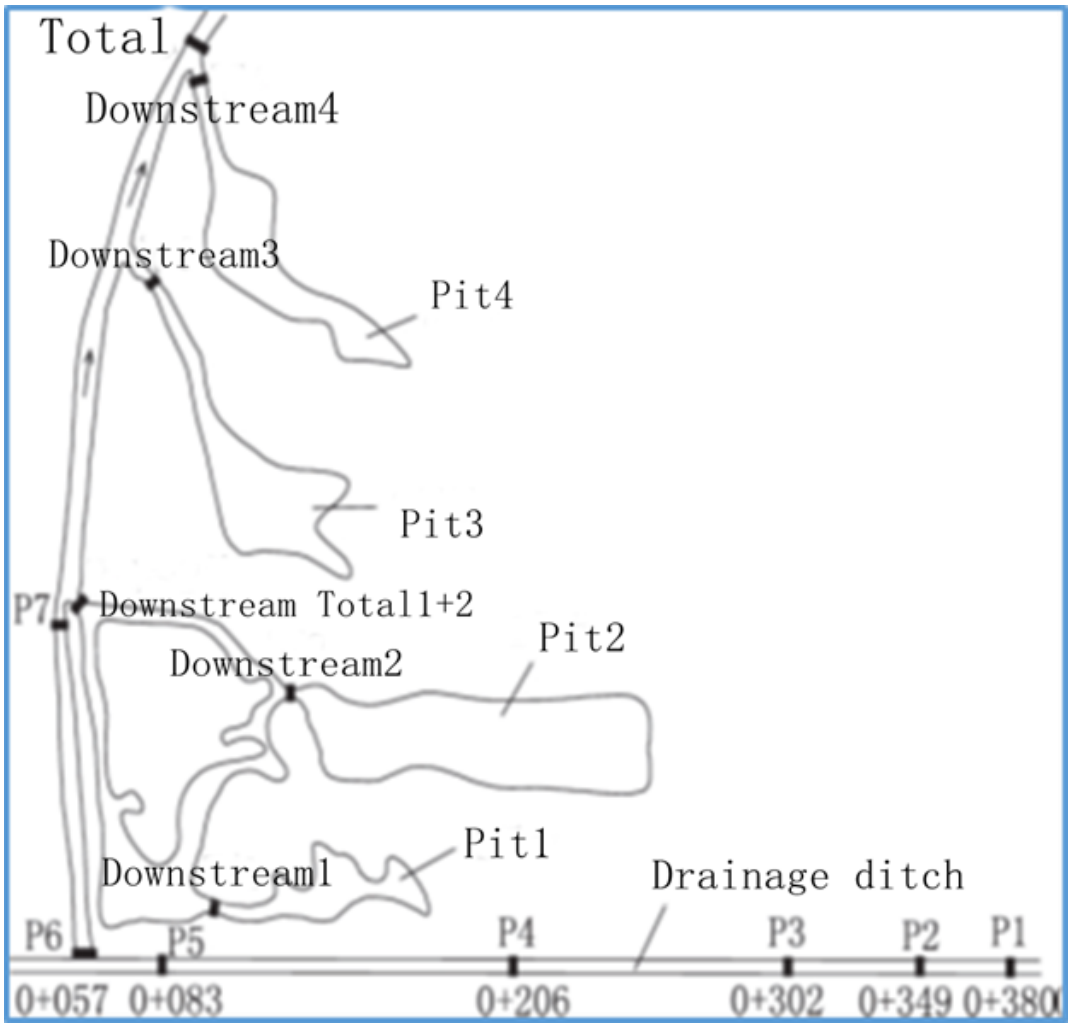

Figure 2: Layout of seepage pits and observation points downstream of the dam

6.2 Seepage Discharge

Based on seepage locations and flow convergence points downstream, 12 discharge observation points were established. Flow was measured using triangular and rectangular weirs (see Figure 2). Over one month of observation, the surface seepage discharge ranged from 47.21 to 64.70 L/s, with an average of 55.08 L/s.

6.3 Analysis of Seepage Modes

(1) Subsurface flow seepage: Caused by the presence of a poorly graded sandy permeable layer of significant thickness in the riverbed foundation.

(2) Seepage through the dam's impervious element: Heterogeneous permeability exists in the clay core, with 44% of samples exceeding the code requirement (1×10^{-5} cm/s) and 17 groups below the design permeability standard (3.6×10^{-6} cm/s).

(3) Seepage through the concrete cutoff wall: The clay core is underlain by the concrete diaphragm wall. Defects were found in the cutoff wall during the investigation.

(4) Seepage through the dam foundation rock mass: Apart from the weathered and fractured surface zone with relatively strong permeability, the overall permeability of the foundation rock is weak. Water pressure tests showed rock permeability rates (Lu values) ranging from 1.5 to 33 Lu, averaging 8.3 Lu, with some sections having higher rates.

(5) Seepage around the dam abutments (abutment seepage): The permeability of the abutment rock mass ranges from 1.5 to 6.8 Lu, indicating weak permeability, but seepage issues nonetheless exist.

6.4 Analysis of Seepage Causes

Analysis of the downstream seepage discharge observations reveals the following patterns:

(1) The maximum seepage discharge in the downstream drainage ditch is located in the dam section from stake 0+000 to 0+083.1, followed by the section from 0+083.1 to 0+205.8. This area corresponds to the main river channel, which has the thickest overburden and the largest hydraulic head difference between the reservoir and downstream, hence the larger seepage. Seepage is relatively smaller in sections 0+349.1–0+380.3, 0+205.8–0+349.1, and 0+380.3–0+505. These sections are on the sides of the main channel where the ground elevation is higher and the head difference is consequently reduced. This observation aligns with the fundamental principles of seepage flow.

(2) Downstream seepage flow is concentrated in the drainage ditch, the main downstream river channel, and Seepage Pits 1, 2, and 3, located 60–240 m from the dam axis. These account for 95.04% of the total observed surface seepage. Seepage Pit 4, located farther away at 245–345 m from the dam axis, shows a significant decrease in flow (2.73 L/s), accounting for only 4.96% of the total. This demonstrates that seepage is distributed within a limited zone downstream of the dam and that the discharge diminishes with increasing distance from the reservoir. This pattern conforms to the principle that seepage decreases as the seepage path length increases.

(3) The lowest terrain is near the main river channel, acting as a natural collector for seepage water. Consequently, further downstream, as more drainage channels converge, the cumulative surface flow increases.

(4) Field surface observations only capture the visible surface flow. Due to the considerable thickness of the poorly graded sandy permeable layer in the riverbed, a significant amount of subsurface (groundwater) flow is also expected to exist.

7. Seepage Discharge Calculation and Prediction

7.1 Analysis and Calculation of Subsurface Flow

Based on the geological cross-section, the thickness of the poorly graded sand layer in the dam foundation ranges from 8.1 to 18.2 m. The distance L between observation point P6 (elevation 1236.65 m) in the downstream drainage ditch and point X4 (elevation 1233.70 m) is 276 m (Figure 2). The ground head difference ΔH is 2.95 m, resulting in an estimated subsurface hydraulic gradient i of 0.0107.

During the investigation, 32 permeability tests on the poorly graded sand yielded coefficients k ranging from 9.05×10^{-6} to 1.76×10^{-4} m/s. For seepage calculation, a representative k value of 3×10^{-4} m/s was adopted. From the dam axis profile, the estimated cross-sectional area A of the poorly graded sand layer is 6100 m^2.

The subsurface seepage discharge Q was estimated using Darcy's law:

$$Q=k\times(\Delta H/L)\times A \quad (1)$$

where Q is the seepage discharge (m^3/s), k is the permeability coefficient (m/s), ΔH is head difference (m); L is seepage path length (m); A is cross-sectional area (m^2).

The calculated subsurface flow discharge Q is 0.01956 m^3/s (19.56 L/s), which accounts for approximately 35.51% of the observed average surface flow.

During the investigation period, the maximum observed surface flow was 84.08 L/s. Adding the estimated subsurface flow gives a total seepage discharge of 103.64 L/s.

7.2 Seepage Calculation for the Clay Core

Fifty permeability tests on core clay samples gave coefficients ranging from 1.66×10^{-7} to 1.85×10^{-4} cm/s, with an average of 2.78×10^{-5} cm/s and a large-value average of 3.64×10^{-4} cm/s.

For calculation, a conservative permeability coefficient of 8.0×10^{-5} cm/s was used. Other parameters included an average core width (thickness) of 9.2 m, a base elevation of 1236.6 m, a dam length of 628 m, and a head difference (ΔH) ranging from 0.00 to 9.79 m at the reservoir level of 1246.79 m.

Applying Darcy's law (Equation 1), the estimated seepage through the clay core (Q_1) at the investigation water level is 1.48 L/s.

If the reservoir impounds to its normal level of 1255.5 m, the corresponding core seepage (Q_1') is predicted to be 6.97 L/s.

7.3 Seepage Calculation for the Concrete Cutoff Wall

Concrete is generally considered impervious. However, considering potential difficulties in achieving perfect embedment into bedrock and the defects identified during investigation, seepage through the wall was assumed. For calculation, a hypothetical 0.5 m thick "permeable layer" within the wall was considered, with an assigned permeability coefficient k of 6×10^{-4} m/s.

At the investigation reservoir level (1246.79 m), the head difference ΔH is 9.79 m. The estimated seepage through the cutoff wall (Q_2) is 72.98 L/s.

At the normal impoundment level (1255.5 m, ΔH = 18.5 m), the predicted seepage (Q_2') increases to 74.27 L/s.

7.4 Seepage Calculation for the Dam Foundation Rock Mass

Water pressure tests showed rock permeability rates (Lu values) of 1.5–33 Lu (avg. 8.3 Lu). Apart from the weathered surface zone, the overall permeability is weak. The deeper fresh rock is intact with few discontinuities and is treated as a relatively impervious layer. For calculation, only the upper 15 m of rock was considered, with a permeability coefficient k of 5×10^{-6} m/s.

At the investigation water level (ΔH = 9.79 m), the estimated seepage through the foundation rock (Q_3) is 18.25 L/s.

At the normal water level (ΔH = 18.5 m), the predicted seepage (Q_3') is 43.57 L/s.

7.5 Seepage Calculation for Abutment Seepage

Abutment rock permeability ranges from 1.5 to 6.8 Lu (weak permeability). The abutment seepage discharge (Q_4) was calculated using the standard formula for seepage around an abutment (specific formula omitted here for brevity). A permeability coefficient k of 5×10^{-6} m/s was used in the calculations.

$$Q = 0.366 \cdot K \cdot H \cdot (H_1 + H_2) \cdot lg\frac{B}{r_0}$$

Q: Total seepage of the left dam foundation (m^3/d); K: Permeability coefficient of the aquifer (m/d); H: Head difference between upstream and downstream (m); H_1: Elevation difference from the top of the relatively impermeable layer to the normal pool level (m); H_2: Elevation difference from the top of the relatively impermeable layer to the downstream water level (m); B: Length of the seepage bypass zone upstream of the dam (m); R_0: Minimum radius of seepage around the dam abutment (m).

In calculations, k is taken as 5×10^{-6} m/s. At reservoir level 1246.79 m, abutment seepage Q_4 is 7.83 L/s. At the normal impoundment level (1255.5 m), the predicted abutment seepage (Q_4') is 16.47 L/s.

Summary of Calculated Seepage: At reservoir level 1246.79 m: Total calculated seepage is 100.54 L/s. At normal impoundment level 1255.5 m, Total predicted seepage is 241.28 L/s.

8. Analysis and Discussion

8.1 Comparison of Observed and Calculated Seepage Discharge

During the investigation, the components of the observed total seepage were as follow: Maximum observed surface flow: 84.08 L/s; Estimated subsurface flow:19.56 L/s; Total Observed Seepage: 103.64 L/s.

The itemized calculation for seepage through all impervious elements at the investigation water level yielded: Clay core (Q_1): 1.48 L/s; Cutoff wall (Q_2): 72.98 L/s; Foundation rock (Q_3): 18.25 L/s; Abutment seepage (Q_4): 7.83 L/s; Total Calculated Seepage: 100.54 L/s.

The calculated total (100.54 L/s) is very close to the observed total (103.64 L/s), with an error of only 3.08%. This close agreement validates the reliability of the estimated permeability parameters and the applied calculation methodology.

8.2 Prediction Analysis of Reservoir Seepage Discharge

Through over three months of comprehensive investigation, the locations of defects in the dam's impervious elements and the primary causes of seepage were identified. The permeability coefficients for key elements were determined.

The successful validation of the calculated discharge against observations confirms the feasibility of the selected parameters and method. Extending this model predicts that the total dam foundation seepage will reach 241.28 L/s (868.61 m_3/h) when the reservoir is at the normal impoundment level of 1255.5 m.

The seepage issue is significant. It is noteworthy that seepage treatment works were conducted in 2015, resulting in a noticeable reduction in downstream seepage. The predicted seepage at the normal level represents about 12.44% of the main river's long-term average annual runoff (1.94 m^3/s), a considerable proportion that would impact the effective water supply of the reservoir. Furthermore, the presence of considerable poorly graded sand within the permeable layer indicates a potential risk of seepage deformation (internal erosion) under sustained seepage flow.

9. Conclusion

Reservoir seepage involves complex multi-field coupling and geological heterogeneity, making its accurate quantitative assessment a persistent challenge in engineering geology. A key difficulty lies in overcoming the spatial variability of permeability parameters in impervious elements and the representational limitations of traditional investigation

methods.

This study demonstrates that the accuracy of parametric representation and the physical authenticity of the computational model are the main sources of uncertainty in seepage prediction. Building upon this understanding, a systematic case study was conducted, leading to the development of a novel investigation methodology. This methodology is characterized by its "air-ground synergy" and a unified "diagnosis-verification integration" process.

The approach emphasizes using multi-scale geophysics to spatially constrain seepage anomalies, followed by precise drilling and in-situ testing to reveal key hydrogeological parameters. Finally, it employs dynamic feedback verification between observation data and theoretical models to establish a self-validating diagnostic loop.

Practical application has shown that this integrated framework not only significantly improves the identification accuracy of complex seepage pathways and the reliability of quantitative predictions but also carries deeper implications. It provides a replicable and generalizable analytical paradigm for achieving a more transparent understanding of seepage systems in earth-rock dams and for implementing risk-controllable engineering interventions.

References

[1] Qiu Yiyuan. Application of High-Density Electrical Method in Reservoir Dam Seepage Detection [J]. Yunnan Water Power, 2025, 41(07): 55-58.

[2] Liu Haiyang, Li Feng, Tang Wanjin. Application of High-Density Electrical Method in Seepage Detection of Dangerous Reservoirs [J]. Yangtze River, 2024, 55(S2): 130-133. DOI:10.16232/j.cnki.1001-4179.2024.S2.023.

[3] Yao Jihua, Wu Youlun, Song Zilong, et al. Study on Identification of Seepage Defects in Plastic Concrete Cut-off Wall of Dams Using Ground Penetrating Radar and High-Density Electrical Method [J]. Chinese Journal of Engineering Geophysics, 2023, 20(05): 599-604.

[4] Zhao Mingjie, Yu Dong, Zhao Huoyan. Experimental Study on Joint Imaging Diagnosis of Wave Velocity and Electrical Resistivity for Seepage in Earth-Rock Dams [J]. Journal of Hydraulic Engineering, 2012, 43(01): 118-126. DOI:10.13243/j.cnki.slxb.2012.01.016.

[5] Wang Risheng. Study on Three-Dimensional Electric Field Distribution and Seepage Diagnosis of Earth-Rock Dams [D]. Chongqing Jiaotong University, 2019. DOI:10.27671/d.cnki.gcjtc.2019.000036.

[6] Zhang Xin, Zhao Mingjie, Wang Kui. Experimental Study on Three-Dimensional Electrical Resistivity Imaging Diagnosis of Seepage in Earth-Rock Dams [J]. Water Resources and Power, 2016, 34(08): 94-98. DOI:10.20040/j.cnki.1000-7709.2016.08.023.

[7] Peng Bo, Zhang Dexuan. Study on Detecting Concentrated Seepage in Earth-Rock Dams Using Infrared Thermography Technology [J]. Science Technology and Engineering, 2016, 16(11): 93-98+103.

[8] Zhang Huajun, Hua Guiqian, Han Zhaoyu, et al. Research on Identification of Hidden Seepage Hazards in Reservoir Dams and Levees Based on Time-Domain Transient Electromagnetic Method [J]. Technical Supervision in Water Resources, 2025, (08): 169-171+332.